Agricultural Systems 193 (2021) 103213

Contents lists available at ScienceDirect

Agricultural Systems

journal homepage: www.elsevier.com/locate/agsy

A GIS-based framework for local agricultural decision-making and regional crop yield simulation

Runwei Li [a,*,1], Chenyang Wei [b,1], Mahnaz Dil Afroz [a], Jun Lyu [c], Gang Chen [a]

[a] Department of Civil and Environmental Engineering at FAMU-FSU College of Engineering, Florida State University, Tallahassee, FL 32310, USA
[b] Department of Geography at College of Arts and Sciences, University at Buffalo, State University of New York, Buffalo, NY 14261, USA
[c] Department of Business Analytics, Information Systems and Supply Chain at College of Business, Florida State University, Tallahassee, FL 32306, USA

HIGHLIGHTS

- A regional crop simulation framework was proposed by coupling CropSyst with GIS.
- Major crops' annual yields were predicted for a cropland-concentrated sub-watershed.
- Low organic matter content and soil sand percentage caused nitrogen deficiency.
- Crop yields could be effectively improved with the tested management strategies.

GRAPHICAL ABSTRACT

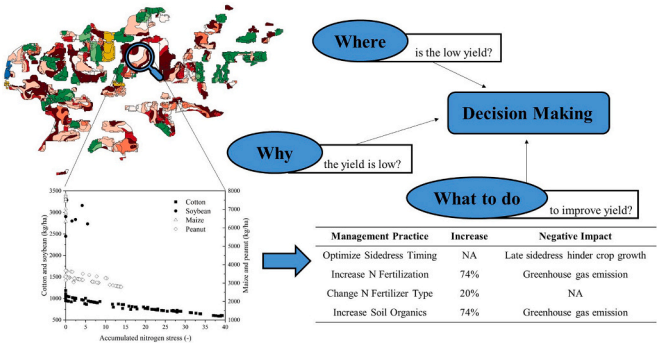

ARTICLE INFO

Editor: Mark van Wijk

Keywords:
CropSyst
Crop yield
Decision-making
GIS
Nitrogen deficiency

ABSTRACT

CONTEXT: In agricultural activities, the decision-making process is central to agricultural system management and subsequent crop yield. As a powerful tool in field-specific decision-making processes, crop simulation models have the potential to simulate crop yields on a large scale. However, their performance is often biased by the spatial heterogeneity of environment and management factors when applied over a large scale.
OBJECTIVE: The major objectives of this study include: (1) Predicting and evaluating the annual yields of dominant crops with real rotation scenarios; (2) Locating fields with low crop yield and determining possible reasons; and (3) Evaluating the improvement for crop yield with different management strategies.
METHODS: This study proposed a crop yield simulation framework at the regional level by coupling a cropping system model (CropSyst) with a geographic information system (QGIS) to provide more reliable information for the decision-making process. In the study of a cropland concentrated USGS sub-watershed (Hydrologic Unit Code: 031402030101) in Geneva County, Alabama, we estimated the annual yields of four regionally dominant crops (i.e., corn, cotton, soybean, and peanuts) from 2016 to 2018. Low yield fields were identified in the simulation results visualization. Moreover, four management strategies were tested at a field scale to improve annual yields.

* Corresponding author.
E-mail address: rl16h@my.fsu.edu (R. Li).
[1] These authors contributed equally to this study.

https://doi.org/10.1016/j.agsy.2021.103213
Received 8 September 2020; Received in revised form 20 June 2021; Accepted 21 June 2021

RESULTS AND CONCLUSIONS: Overall, the simulated crop yields were significantly correlated with the recorded values (Pearson's $r = 0.99$). However, the performance of the regional model varied for different crops. The model achieved the best performance for soybean with a high index of agreement (0.93) and modeling efficiency (0.86). For cotton, the model achieved positive model efficiency (0.23) and a good index of agreement (0.59). For peanut and maize, the model fitted records well but not sensitive enough. According to the visualization of simulation results, we located fields with low yields. The low organic matter content and high sand percentage of the soil were the potential causes of the nitrogen deficiency, which leads to the low yield subsequently. In field scale tests, four proposed management strategies could increase the cotton yields as high as 74.4%. But some strategies would also increase greenhouse gas emissions at the same time.
SIGNIFICANCE: This study bridges the gap between local cropping system models and the regional estimation of crop yields. The GIS-based crop simulation framework developed here demonstrates the potential of cropping system models to provide reliable information at a regional scale and hence significantly broadens their application in the agricultural decision-making process.

1. Introduction

Decision-making is a selection among several alternatives based on values, possibilities, and personal preferences (Isen et al., 1982; Dietrich, 2010). In agricultural activities, the decision-making process is ubiquitous in cropland-related management, such as irrigation, fertilization, tillage, harvest, and residue treatment. One of the essential factors for agricultural decision-making is the maximization of farmers' profit (Feather and Cooper, 1995; Perez, 2015), which leads to reluctance to accept potential risks. For example, some farmers still rely on a high dosage of fertilizer due to their concern about production loss (Stuart et al., 2014), even though increasing fertilizer efficiency rather than dosage would contribute to achieving economic optimum (Smith and Siciliano, 2015). A supporting system providing accurate crop yield prediction would ensure that farmers have rational risk perceptions and could play a critical role in profit maximization (Foster and Rausser, 1991; Dury et al., 2012).

Model simulation has been widely used to study agricultural activities for a long time (Bouman et al., 1996; Hansen, 1996). As an essential tool to quantitatively characterize an agricultural system, model simulation can integrate different dynamic processes associated with crops, soil, climate, and human activities (Zhang et al., 2002). The first crop growth model was developed by de Wit back in the 1960s, and it simulated photosynthesis of leaf canopies by combining physical and biological principles (de Wit, 1958; de Wit, 1965). Beginning with the work from pioneers, the evolution of agricultural modeling was boosted by increasing grant opportunities from the public and private sectors and the revolution in related technologies (Jones et al., 2017). Over more than six decades, numerous agricultural system models have been developed for different end-users with specific purposes. For examples, DSSAT and CropSyst are used for modeling the crop growth and yield; ADEL and OpenAlea are used for virtual plants simulation; DNDC and DayCent are used to simulate greenhouse gas emission from agriculture fields; agent-based models are used in the simulation of agricultural economics (Parton et al., 1998; Zhang et al., 2002; Fournier et al., 2003; Parker et al., 2003; Stöckle et al., 2003; Pradal et al., 2008). Although the focuses of these modeling efforts are quite different, all of them help to understand the interaction between agricultural production, natural resources, and human factors.

Previous studies have demonstrated that crop simulation models successfully estimate the crop yield and the impact of different management strategies at field-specific scales for most of the cash crops in the U.S., such as maize, soybean, and cotton (Farahani et al., 2009; Setiyono et al., 2010; Liu et al., 2011; Archontoulis et al., 2014). With accurate information about crops, soil, and weather, crop simulation models can be applied to investigate the temporal variation of crop yield at a scale where environmental conditions are relatively homogeneous (Florin et al., 2009; Balkovič et al., 2013). However, in the decision-making process, decision/policy makers often need the upscaled information at larger spatial extents where the crop model simulation is often biased by the spatial heterogeneity in soil distribution, climate pattern, and human preference in rotation and management (Hansen and Jones, 2000; Priya and Shibasaki, 2001).

To enlarge the scale of crop simulation, geographic information system (GIS) is technically necessary due to its ability to store, manipulate, analyze, and visualize the relevant spatial data (Maguire, 1991; Hartkamp et al., 1999). With the aid of GIS, crop simulation can be applied over various scales. At relatively large extents (e.g., national and global), GIS-based crop models are usually used to investigate the response of agricultural systems to environmental stress. Liu (2009) applied GEPIC model, the combination of ArcGIS and EPIC crop model, to investigate the relationship between water management and crop production at a global scale. Parry et al. (2004) analyzed the global impact of climate change on crop production by integrating geospatial input with a crop growth model (i.e., IBSNAT-ISACA). Large extent applications are usually suffered from low resolution of input data and cannot capture the spatial variation within modeling units. On the other hand, GIS-based crop simulation applications at relatively small extents (e.g., field to regional) usually study the impact of field variability (e.g., soil, cultivar, and management practices) on crop yield. Thorp et al. (2008) developed an interface (i.e., Apollo), combing ArcGIS and DSSAT crop growth model, to evaluate the impact of management practices and environmental factors on crop yield at a field scale. Jin et al. (2017) estimated wheat yield at a regional scale with remote sensing data and AquaCrop crop model. Compared to the application at large extents, GIS-based crop simulation at small extents could take advantage of fine resolution inputs and better support decision-making processes in specific agricultural systems.

No matter the scales, current GIS-based crop simulation studies tend to simplify or neglect crop modeling inputs, especially management practices which vary greatly over space and time. Among those practices, rotation is often excluded from the consideration. Integrating crop rotation into the simulation requires a great modeling effort since agricultural land uses (e.g., crop species, crop proportion, and field area) often changes constantly even in a single field. In addition, the degree of this variation is highly dependent on the field owner's personal preference and experience, which would also introduce a large spatial variation. Due to these difficulties, existing GIS-based crop simulation studies mostly focused on single-year and single-crop analyses (Thorp et al., 2008; Resop et al., 2012; Kadiyala et al., 2015; Jin et al., 2017). However, crop rotation is regarded as a prominent strategy to increase the sustainability of agricultural systems and is widely applied all over the world. Kollas et al. (2015) indicated that, compared to the simulation of single years and single crops, the simulation of multi-year crop rotations provided more reliable results with fewer errors at specific fields in Europe. Among previous GIS-based crop simulations, only a few studies considered crop rotation with simplification. Zhang et al. (2010) evaluated biofuel crop production from 10 assumed crop rotations in several counties in Michigan State. Morari et al. (2004) studied the impact of fertilization and irrigation on crop production at a sub-watershed scale, in which the rotation is simplified by assuming the major crop (i.e., the

crop with the largest cropping area) as the only crop in a modeling unit.

In this study, a crop growth model is jointed in a GIS-based framework to simulate the crop yield at a sub-watershed scale. Among various types of crop growth models, CropSyst (version 4) (Stöckle et al., 2003) is selected since this processes-based crop model can easily generate a combination of predefined input factors (i.e., soil, weather, management practices, and crop rotation) through its scenario generator. On the other hand, given its open-access toolbox and easy-to-use interface, the QGIS (version 3.6.3) platform (QGIS Development Team, 2016) is selected for inputs preparation and outputs visualization in this study. Compared with previous GIS-based crop simulation, this study applied more realistic crop rotations, which would contribute to a more reliable prediction. Subsequently, the framework developed in this study would better bridge the gap between local cropping system models and the regional estimation of crop yields. Our major objectives include: (1) Predicting and evaluating the annual yields of dominant crops at an agricultural-land-concentrated sub watershed; (2) Locating fields with low crop yield and determining their possible reasons; and (3) Evaluating the improvement for crop yield with different management strategies in testing scenarios.

2. Method

2.1. CropSyst-GIS framework

A GIS-based framework was established to investigate the crop yield simulation at a regional scale (Fig. 1) (Hartkamp et al., 1999; Stöckle et al., 2003). This framework consisted of a crop simulation model and a GIS platform. The CropSyst (version 4), a multi-year multi-crop daily time-step model, was used to simulate crop yield, while the QGIS (version 3.6.3) software was used for preparing model inputs and visualizing simulation outputs (Stöckle et al., 2003, QGIS Development Team, 2016). Based on the combination of different types of local information (i.e., rotation scenarios, soil types, and weather), the study area was segmented into different polygons, in which modeling inputs were homogeneous. And, crop yields simulation was conducted by the CropSyst (version 4) within each polygon. The simulation results were then visualized for all the polygons according to the predicted annual yields of corresponding crops.

For each crop, the simulated yields were divided into five categories, namely below 60%, 60 to 70%, 70 to 80%, 80 to 90%, and beyond 90% of the maximum recorded yields (i.e., 1102 kg/ha, 3807 kg/ha, 8742 kg/ha, and 3255 kg/ha for cotton, peanut, maize, and soybean, respectively) in the study area (USDA-NASS, 2003). The polygons with crop yields less than 60% of the maximum records were regarded as low yield polygons. In this study, a nitrogen stress index (NSI) was computed daily by the CropSyst (version 4) to quantify the plant response to nitrogen deficiency condition. The NSI ranges from 0 to 1 with higher values indicating greater nitrogen stress in crop growth (Stöckle et al., 2003). The daily NSI values were then summed for each year to represent the annual accumulation of nitrogen stress.

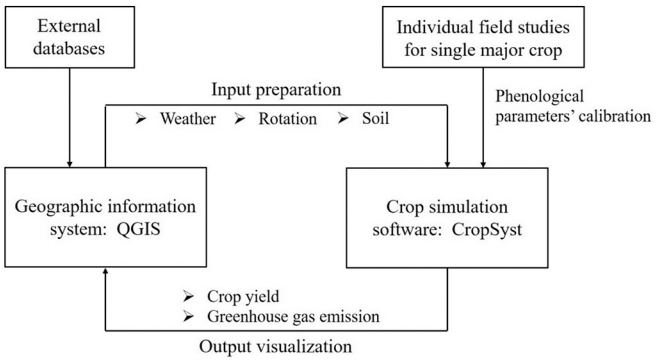

Fig. 1. GIS-based framework for the regional crop yield simulation.

Two assumptions underlay the framework. First, the deterministic field crop simulation is also valid at a regional scale. According to the development of modeling units (i.e., polygons), modeling inputs within each unit are homogenous. Therefore, crop growth modeling in each unit is reliable and the overall performance of the framework depends on the accuracy of modeling inputs. Second, the physical transferring processes between neighboring modeling units are neglected. Two possible transferring processes include runoff water and contained nutrients. Runoff water can be neglected here since water demand is easily satisfied by rainfall. Nutrients in runoff water could be an extra input. However, runoff water from the neighboring field will pass on until reach a drain in a sequence of fields.

2.2. Study area

By incorporating the National Watershed Boundary Dataset, a cropland-concentrated USGS sub-watershed (Hydrologic Unit Code: 031402030101) near the City of Hartford, Alabama, was selected as the study area (U.S. Geological Survey, 2019) (Fig. 2). The total area of the selected sub-watershed was around 24.86 km^2, in which agricultural land use accounted for approximately 82%. Based on the annual geospatial information of cropland from the U.S. Department of Agriculture (USDA, 2019), five dominant agricultural land uses were defined in the study area from 2016 to 2018, namely cotton, peanuts, maize, soybean, and fallow. Each selected land use accounts for over 5% of the total agricultural area in at least one of the three years. Among the five land uses, cotton and peanuts are the most dominant land uses. Together, they account for more than 67%, 78%, and 91% of the total agricultural area in 2016, 2017, and 2018, respectively. The cropping area of each selected land use is summarized in Supplementary Materials (Table S1). According to local weather, rotation scenarios, and soil types, the studied area was segmented into 904 polygons with each polygon containing uniform local variables in each year.

2.3. Rotation

For the study area, the annual geo-referenced and agricultural land-cover datasets from 2016 to 2018 were downloaded from the CropScape Crop Data Layer (CDL) database as raster files (USDA, 2019). Besides the five dominant land uses, the raw raster datasets also included other trivial agricultural lands (e.g., sugarcane, wheat, and oats) and non-agricultural land uses (e.g., forest, water, and developed area). These non-interest areas were reclassified as a land-cover type of "null" to obtain annual cropland maps with only the dominant land uses. The generated annual raster files were then vectorized as polygons in QGIS (version 3.6.3). Since the CDL datasets were developed based on the classified LANDSAT satellite imagery at a moderate resolution (30 m), some polygons in the obtained cropland maps may not be precisely located within agricultural fields. Therefore, only polygons with an area over 4 LANDSAT pixels (0.0036 km^2) were selected from the annual cropland maps. Then, by overlaying all the annual cropland maps together, a dataset containing all dominant rotation scenarios was generated for the years from 2016 to 2018. Specifically, 85 crop rotation scenarios were obtained from historical records in the study area. Based on the dataset of rotation scenarios, the individual rotation files were built for the crop yield simulation. The 15 dominant rotation scenarios and their applied percentages are summarized in the Supplementary Materials (Table S2).

2.4. Soil

The soil map of the study area was downloaded from the SSURGO database (Soil Survey Staff, 2019). The primary soil characteristics used in the simulation included soil layers' thickness, texture, organic matter content, permanent wilt point, field capacity, bulk density, water

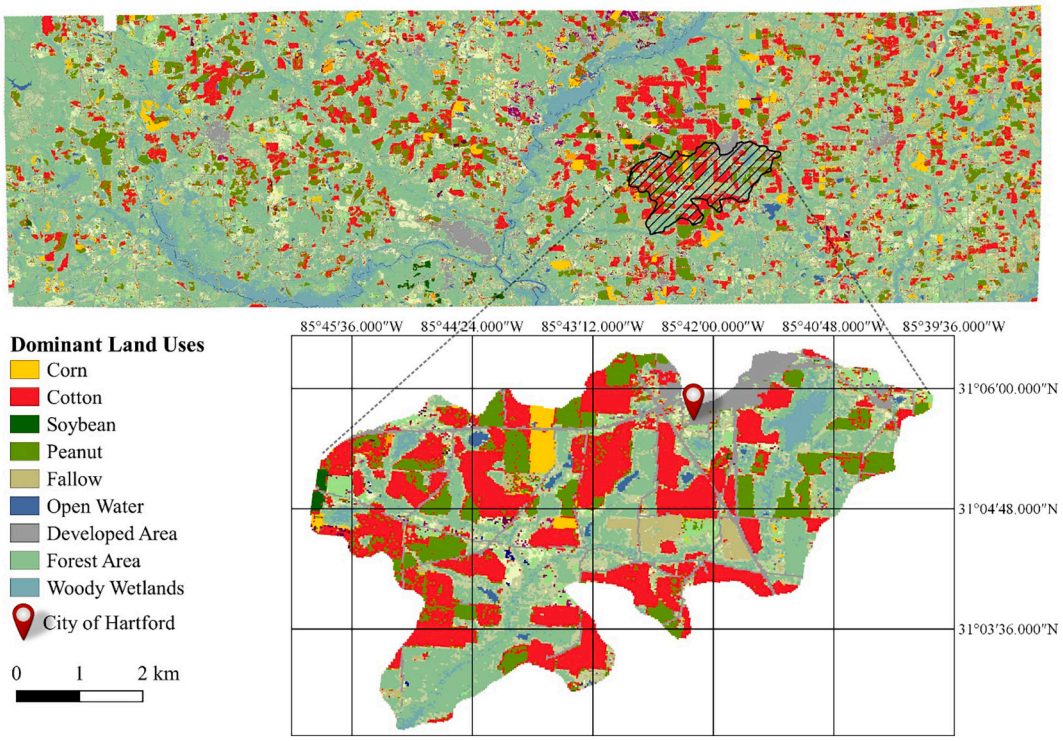

Fig. 2. Dominant Land Use in the Study Area. Note: The land use of 2016 is presented as an example.

potential at field capacity, saturated hydraulic conductance, air entry potential, water saturation, pH value, etc. For the study area, the dominant soil types were Orangeburg sandy loam and Dothan fine sandy loam, which accounted for 50.6% and 44.6% of the total agricultural area, respectively. The critical parameters of the dominant soil types are described in Supplementary Materials (Table S3). By using the soil convertor utility of the CropSyst (version 4), the unique soil files were built automatically prior to the crop yield simulation.

2.5. Weather

The variations of key weather characteristics were less than 2% in the selected sub-watershed (Table S4, Supplementary Materials). Accordingly, the weather information at one location (31°6′N, 85°42′W) within the sub-watered was extracted to represent the local weather condition of the study area. The weather data from 2016 to 2018 were downloaded from the Daymet database (Thornton et al., 2018), which provided gridded estimates of daily weather parameters. The primary weather characteristics included daily maximum temperature, minimum temperature, solar radiation, precipitation, and relative humidity. The daily weather conditions at the selected location were plotted in Supplementary Materials (Fig. S2). Based on the extracted Daymet weather data, an individual weather file was created using the weather converter utility of the CropSyst (version 4).

2.6. Management

There are several significant aspects of the decision-making process in agricultural management, which include rotation, planting date, fertilization, irrigation, harvesting, and tillage. Among these aspects, rotation scenarios were determined for this study through the approach described in Section 2.3. Harvesting was performed five days after crop maturation. The detailed harvesting practices are predefined in the CropSyst (version 4) according to National Resources Conservation Service (NRCS) field operation. Specifically, the harvesting practices for cotton, peanut, and maize could be directly found in CropSyst (version 4) database. For soybean, the harvesting practices for general cover crop were applied. Irrigation was not applied in this study according to the comparison between estimated effective precipitation and reference crop evapotranspiration (Table S5, Supplementary Materials). CropSyst (version 4) allows users to specify fertilizer type and applied nitrogen in the forms of ammonium and nitrate. Since the real management decisions are not accessible, we assumed uniform fertilizer type of urea, which accounts for the largest global fertilizer usage (i.e., 57%) and leads ammonium as the only nitrogen form (Heffer and Prud'homme, 2016). Other critical management decisions, including planting, fertilization schedule, and tillage, were determined based on practical recommendations (Kissel and Sonon, 2008; NASS, 2010; NRCS, 2017) and summarized in the Supplementary Materials (Table S6). A unique management file was built for each major crop as an input dataset for the model.

2.7. Crop calibration

The primary crops' phenological parameters were calibrated before they were used in the simulation. The parameter calibration process was based on the measured total biomass and leaf area index from four published independent field studies, which were performed in the nearby states (i.e., Florida, Georgia, and Mississippi) having a weather pattern similar to the study area (Cherr et al., 2007; Ortiz et al., 2009; Dzotsi et al., 2015; Zhang et al., 2016). For the parameter calibration, model inputs related to soil characteristics and management decisions were directly obtained from the field studies. While the corresponding weather data were downloaded from the Daymet database according to the location of each field study. In the calibration process of each crop, weather, soil, and management input files were generated prior to the crop yield simulation. The rotation was not considered in calibration since all the selected field studies were focused on the growth of a single crop within one year. The critical information of these field studies was summarized in Supplementary Materials (Table S7).

2.8. Statistical evaluation

The calibration process was evaluated by comparing the simulated results with recorded total biomass and LAI. On the other hand, area-weighted average yields were computed for each crop. And the regional simulation performance was evaluated by comparing the average yields with the annual crop yield records of Geneva County, Alabama (USDA-NASS, 2003).

$$P_{i,ave} = \sum_j P_{i,j} \times \frac{A_{i,j}}{\sum_j A_{i,j}} \quad (1)$$

in which, $P_{i,\ ave}$ is the area-weighted average yield of crop i in each year, $P_{i,\ j}$ is the annual yield of crop i in polygon j, $A_{i,\ j}$ is the planting area of crop i in polygon j in each year.

Statistical parameters used in this study include Pearson's correlation coefficient (r), mean error (E), root mean square error ($RMSE$), normalized RMSE ($n\text{-}RMSE$), modeling efficiency (EF), and an index of agreement (d) (Confalonieri et al., 2009; Yang et al., 2014). Each parameter was further described in the Supplementary Materials.

Table 1
Key phenological parameters used in the CropSyst (version 4) simulation.

Parameters (unit)	Cotton	Peanut	Soybean	Maize
Thermal time				
Base temperature (°C)	6.0 (R[1])	6.0 (R)	5.0 (R)	8.0 (R)
Cutoff temperature (°C)	20.0 (R)	24.0 (R)	22.0 (R)	26.0 (R)
Transpiration				
Canopy extinction coefficient for total solar radiation (−)	0.5 (D[2])	0.5 (D)	0.5 (D)	0.5 (D)
Evapotranspiration crop coefficient at full canopy (−)	1.0 (D)	0.8 (C[3])	1.16 (R)	1.20 (R)
Leaf water potential at the onset of stomatal closure (J/kg)	−1100 (R)	−700 (D)	−1000 (D)	−700 (D)
Wilting leaf water potential (J/kg)	−1600 (R)	−1100 (R)	−1500 (D)	−1600 (D)
Maximum water uptake (mm/day)	12.0 (R)	10.0 (R)	12.0 (D)	14.0 (R)
Attainable growth				
Radiation use efficiency (g/MJ)	2.88 (R)	2.20 (R)	4.00 (R)	4.00 (R)
Above-ground biomass transpiration coefficient (Pa)	4.00 (C)	7.50 (C)	6.30 (C)	12.50 (C)
Canopy development				
Max expected leaf area index (m^2/m^2)	10.0 (R)	6.0 (R)	10.0 (R)	5.0 (D)
Specific leaf area at optimum temperature (m^2/kg)	26.0 (C)	24.0 (R)	28.0 (C)	22.0 (D)
Fraction of Max LAI at physiological maturity (−)	0.15 (C)	0.87 (C)	0.63 (C)	0.15 (C)
Stem/leaf partition coefficient (−)	2.30 (C)	2.75 (R)	3.00 (D)	5.50 (C)
Leaf area duration (°C-Days)	750 (C)	1600 (C)	900 (R)	800 (D)
Phenology				
Emergence (°C-Days)	100 (D)	100 (D)	35 (C)	40 (R)
End canopy growth (°C-Days)	996 (D)	1040 (D)	1040 (D)	690 (C)
Begin flowering (°C-Days)	996 (D)	1000 (D)	1000 (D)	650 (C)
Physiological maturity (°C-Days)	1975 (C)	2270 (C)	1800 (C)	1190 (R)
Others				
Max root depth (m)	1.50 (D)	1.50 (D)	1.70 (D)	1.50 (D)
Harvest Index (−)	0.50 (D)	0.40 (R)	0.50 (D)	0.58 (R)

Note: 1. R stands for reference; 2. D stands for default; 3. C stands for calibration.

3. Results and discussion

3.1. Crop parameter calibration

Key phenological parameters (Table 1) were determined based on the literature review about previous crop simulation research. The parameters were classified into five categories (i.e., thermal time accumulation, transpiration, canopy development, phenology, and others) and were determined based on three primary sources: (1) default values provided by CropSyst (version 4), (2) reported values from previous studies, and (3) adjusted values from the parameter calibration process in this study. The calibration process was adapted from previous CropSyst simulation studies (Donatelli et al., 1997; Sommer et al., 2008; Todorovic et al., 2009). Specifically, calibration started with adjusting the thermal time accumulation parameters (i.e., base and cutoff temperature) and phenology parameters (i.e., thermal time to achieve emergence, end of canopy growth, beginning of flowering, and maturity) to guarantee a good match between the simulated and observed phenological stages. Then, other parameters were refined iteratively so that the simulated total biomass and LAI fit well with the observed data. Among all the key phenological parameters, values from model default settings and previously published studies were preferred in the calibration process, while the rest parameters were manually adjusted in a reliable range provided by the CropSyst (version 4).

Fig. 3 shows the parameter calibration for the selected four crops. For all crops, $n\text{-}RMSE$ is less than 15.3%, EF is larger than 0.77, and d is larger than 0.81 (Table 2), indicating a good fitting with acceptable errors (Yang et al., 2014). As displayed in Fig. 4, the simulated values of LAI and total biomass are highly correlated with corresponding measurements, with Pearson's correlation coefficients of 0.979 and 0.980 for LAI and total biomass, respectively. Overall, good agreement was achieved for the selected phenological parameters in the calibration, although differences still existed between the predicted and measured values. Particularly, the calibration of cotton parameters failed to capture the detailed trend of total biomass due to the lack of field measurements (Fig. 3a). Moreover, maize simulation fails to capture the total biomass increase in grain filling period, which may lead to underestimation of yield (Fig. 3d). On the other hand, peanut and soybean simulation have reliable performance. However, the standard deviation of observed data was relatively large. The mean-based calibration may lead to potential errors in later regional simulation. The calibrated phenological parameters were fixed in the regional simulation of annual crop yields.

3.2. CropSyst-GIS performance

The regional simulation of crop yield in the study area is presented in Fig. 5. Simulated yields ranged from 588 to 1187 kg/ha, 2797 to 3676 kg/ha, 6347 to 6846 kg/ha, and 2446 to 3295 kg/ha for cotton, peanut, maize, and soybean, respectively.

As displayed in Fig. 6, the area-weighted average annual yields were compared with the records from 2016 to 2018. Overall, the regional simulation achieved a Pearson's correlation coefficient of 0.99, indicating an overall satisfactory match between simulation and observation. Furthermore, according to the 1:1 line (Fig. 6), the agreement between the simulated and recorded annual yields was relatively high for cotton, peanut, and soybean. However, the simulation underestimated maize yield in 2017 by 1425 kg/ha.

According to the calculated statistical parameters (Table 3), the regional simulation successfully predicted the annual yields of soybean with a small n-RMSE of only 2.2% and a high index of agreement of 0.93. Besides, the corresponding modeling efficiency (0.86) was also close to 1, indicating the significant predictive power of soybean yield simulation. For the simulation of peanut yield, the computed n-RMSE (7.0%) and index of agreement (0.42) were both satisfactory. A negative average error of −240 kg/ha suggested that the recorded peanut yields

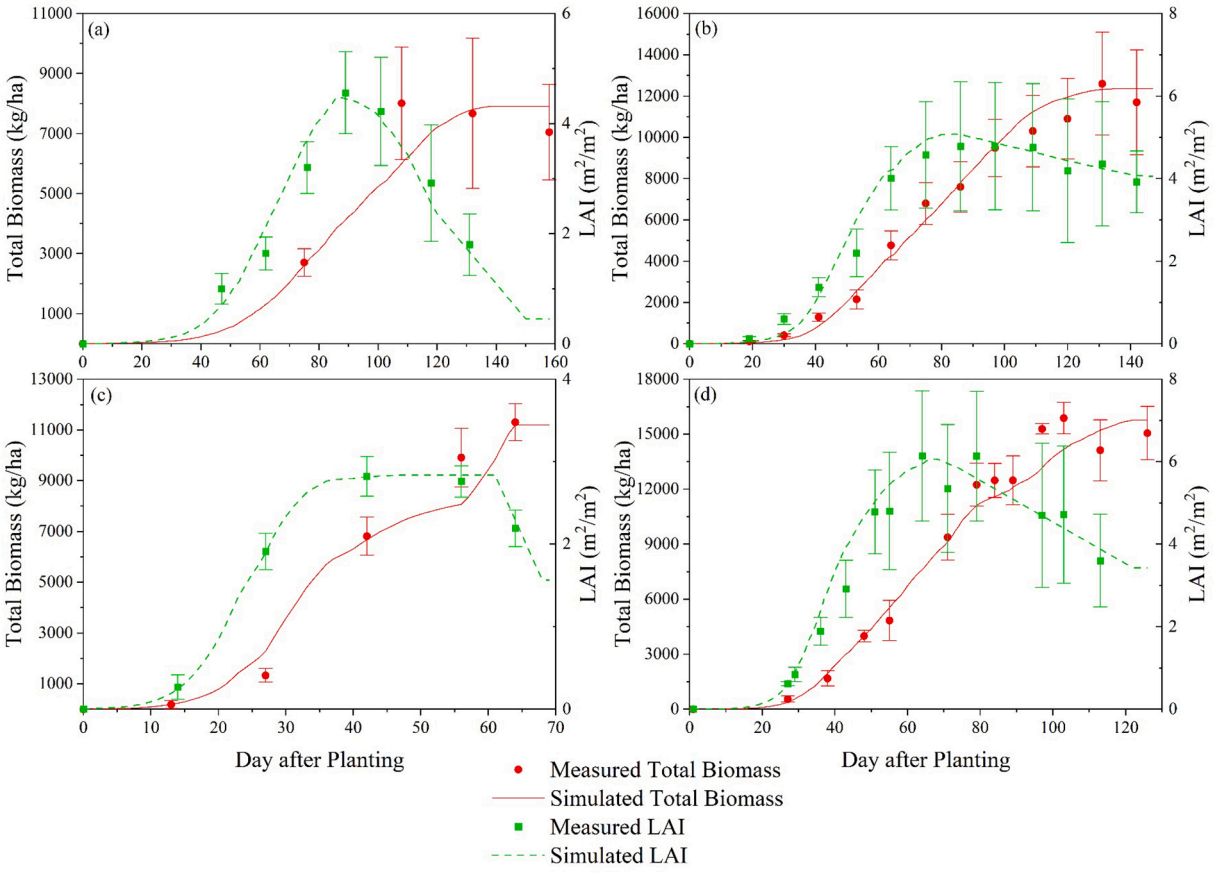

Fig. 3. Critical phenological parameter calibration for the four crops: (a) Cotton, (b) Peanut, (c) Maize, and (d) Soybean.

Table 2
Statistical evaluation for parameter calibration.

Crop	Cotton		Peanut		Maize		Soybean	
	Total Biomass	LAI	Total Biomass	LAI	Total Biomass	LAI	Total Biomass	LAI
RMSE	978	0.31	539	0.30	944	0.13	1302	0.45
n-RMSE	15.3	11.1	8.3	9.9	15.0	8.1	12.3	12.5
EF	0.77	0.88	0.90	0.87	0.86	0.92	0.82	0.81
d	0.81	0.90	0.95	0.94	0.93	0.96	0.91	0.90

were generally higher than the corresponding predicted values. However, the modeling efficiency of peanut yield (−0.40) was less than 0. In this case, due to the small relative standard deviation of the recorded peanut yields (6.0%), the model was not sensitive enough to predict the relatively stable annual yields of peanut in the study area (Moriasi et al., 2007). For the yield simulation of cotton, although the index of agreement was relatively high (0.59) and the modeling efficiency (0.23) was greater than 0.0, the n-RMSE (14.2%) was higher than all the other primary crops. The regional simulation accurately predicted the cotton yields for the first two years and captured the decreasing trend of the measured yields to a certain degree. However, the decrease in the observed cotton yields was more significant than the prediction, which led to a large difference between the simulation and observation in 2018 (i.e., 169 kg/ha). As to the maize, although the regional simulation achieved a satisfactory index of agreement (0.41), it underestimated annual yields of maize in the first two years, especially for 2017 with the difference reaching 1425 kg/ha. The n-RMSE of maize yield simulation was 10.5%, indicating an unsatisfactory match. Moreover, a negative modeling efficiency (−0.11) suggested that the regional model is not sensitive to the yield changes of maize.

3.3. Nitrogen deficiency

As displayed in Fig. 7, the accumulated nitrogen stress in the study area was classified into five categories (i.e., trivial, low, medium, high, and extremely high). In 2016, the summed N_{SI} was close to zero no matter which crop was planted, with the greatest value of only 0.025 in the study area. Since the nitrogen demand was mostly fulfilled, the yield in each polygon reached its maximum with given weather, soil, and management conditions, which also led to evenly distributed yields (Fig. 5a). In the latter two years, nitrogen stress was dramatically piled up in some regions. A general overlap was identified between polygons with relatively high annual nitrogen stress (Fig. 7) and low annual crop yields over the three years, especially in 2017 and 2018 when nitrogen from soil organic matters and fertilizers could not satisfy the demand of crop growth (Fig. 7b and c).

Furthermore, we observed that the accumulated nitrogen stress was closely related to the crop species and soil type. From the aspect of crop species, the nitrogen deficiency often occurred in areas planted with crops having high nitrogen demand, such as cotton. Previous studies have indicated that cotton typically require more than 78 kg N/ha of nitrogen in growing season (Boquet et al., 2004; Kissel and Sonon,

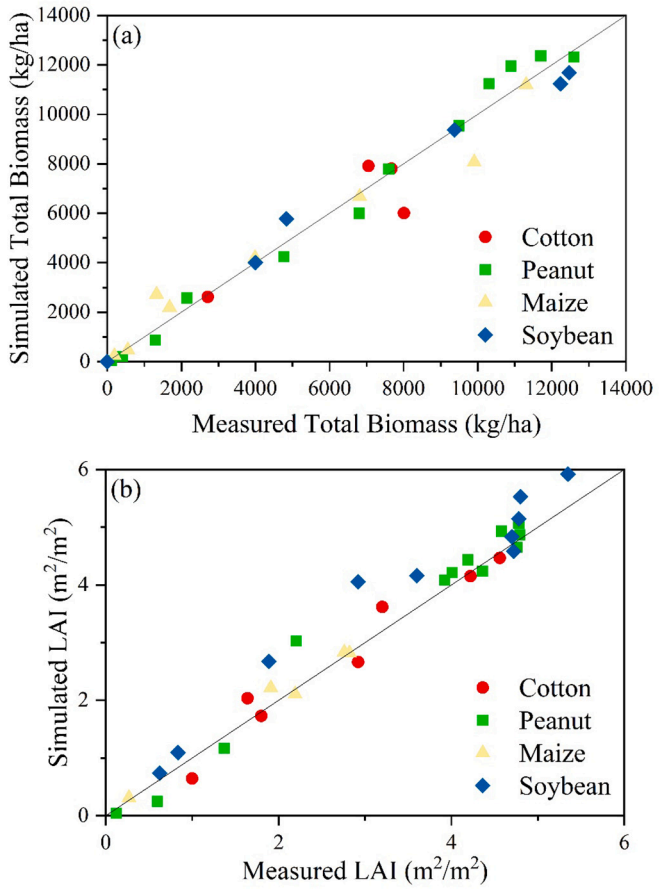

Fig. 4. Comparison between the measured and simulated phenological parameters of the four major crops: (a) Total biomass, and (b) Leaf area index (LAI).

2008). In 2017, there were 87 out of 904 polygons in the study area with at least a medium level of nitrogen deficiency. Among them, polygons planted with cotton, peanut, and soybean accounted for 62.1%, 32.2%, and 5.7%, respectively. In 2018, the number of the same type of polygons increased to 473 with 84.4% of them planted with cotton. Numerous studies have verified that cotton requires a large amount of nitrogen, which plays an essential role in fueling the growth of cotton (Bondada and Oosterhuis, 2001; Dong et al., 2012). As to peanut and soybean, although they can fix nitrogen from the atmosphere, they may also need fertilization when nitrogen from symbiosis cannot satisfy their needs of crop growth and canopy development (Ball et al., 1983; Zhang et al., 2017).

On the other hand, nitrogen deficiency normally happened in regions with relatively low soil fertility. With the lowest organic matter content

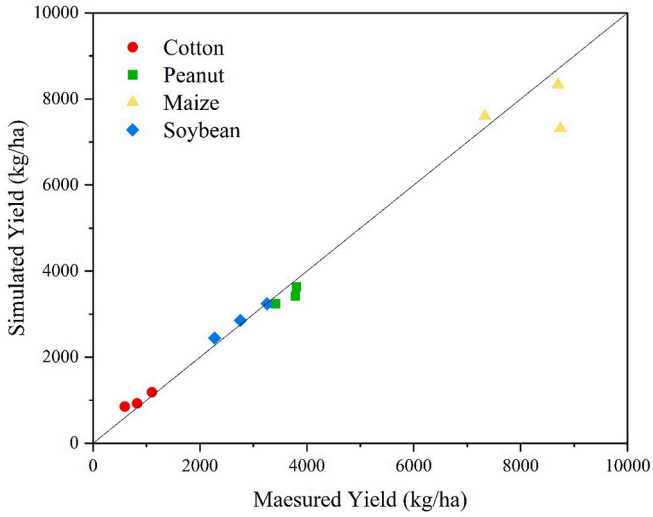

Fig. 6. Comparison between the simulated and recorded annual yields of the four primary crops in the study area.

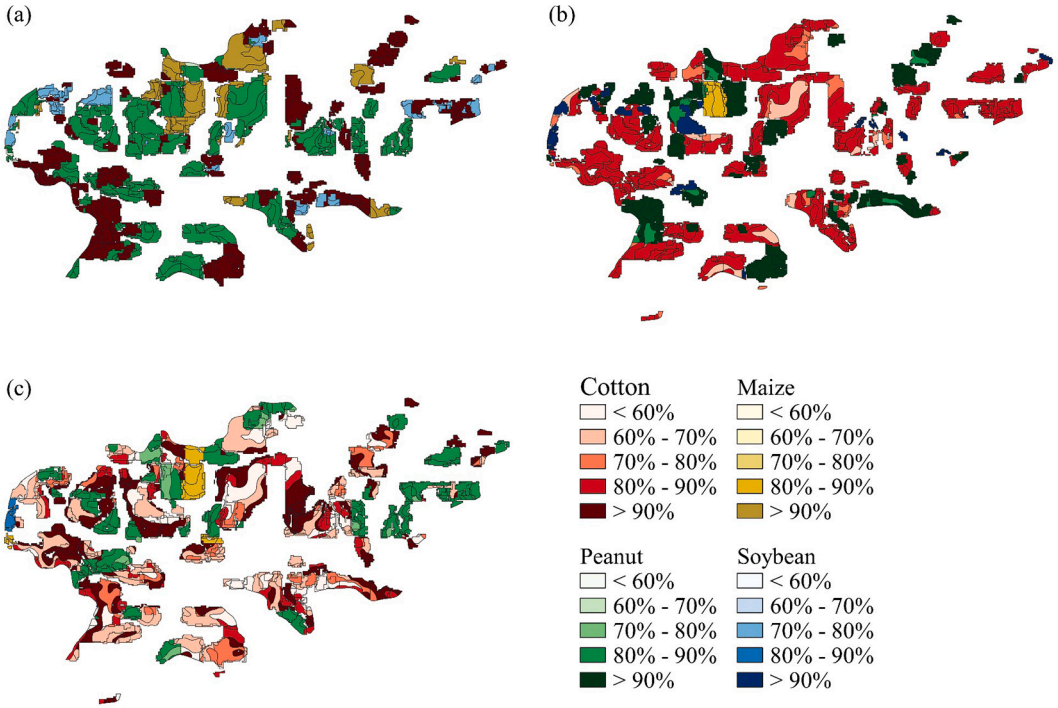

Fig. 5. Regionally simulated yields of the four primary crops in the study area: (a) 2016, (b) 2017, and (c) 2018.

Table 3
Statistical evaluation for the yield simulation of the four crops.

Crop	Recorded yields (kg/ha)			Simulated yields (kg/ha)			E^1 (kg/ha)	$RMSE^2$ (kg/ha)	$n\text{-}RMSE^3$ (%)	EF^4 (–)	d^5 (–)
	2016	2017	2018	2016	2017	2018					
Cotton	1102	824	683	1187	927	851	119	124	14.2	0.23	0.59
Peanut	3787	3807	3411	3416	3628	3242	−240	257	7.0	−0.40	0.42
Maize	8702	8742	7330	8334	7317	7604	−506	864	10.5	−0.11	0.41
Soybean	2273	3255	2757	2246	3238	2856	18	60	2.2	0.86	0.93

Note: 1. *E* stands for mean error; 2. *RMSE* stands for root mean square error; 3. *n-RMSE* stands for normalized root mean square error; 4. *EF* stands for modeling efficiency; 5. *d* stands for index of agreement.

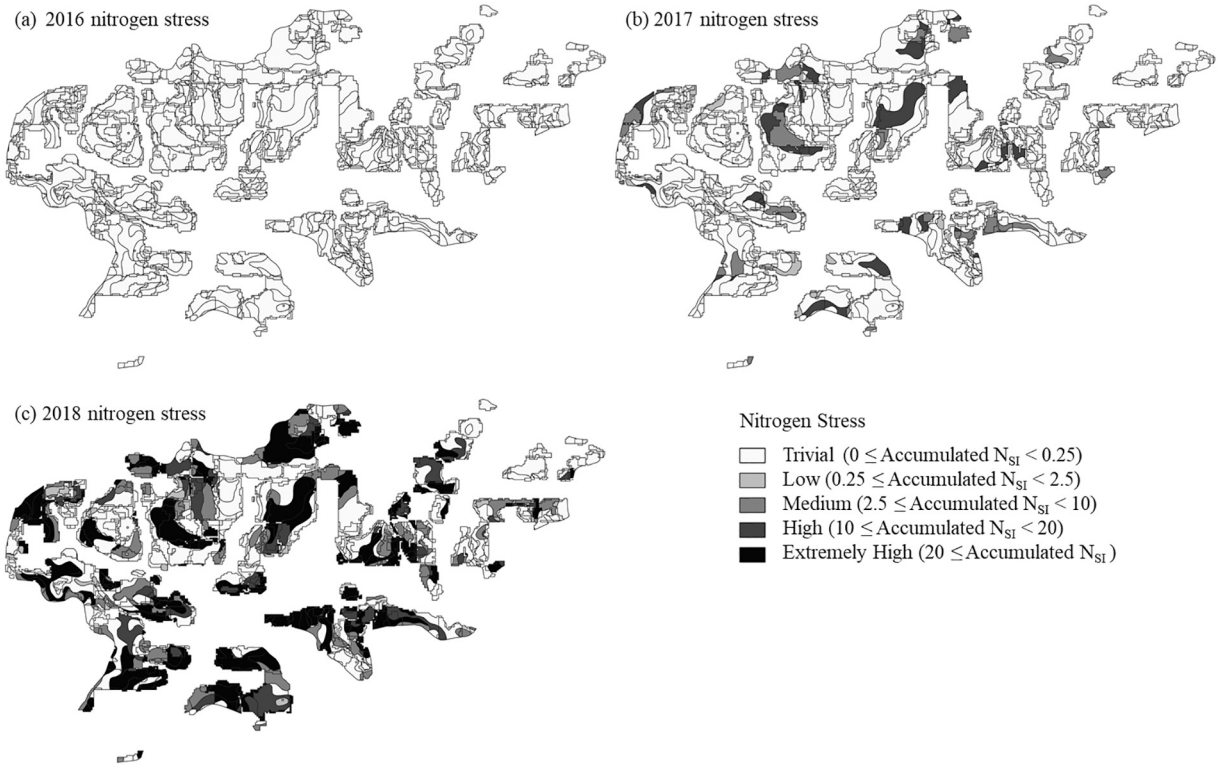

Fig. 7. Annually summed nitrogen stress indices (N_{SI}) of each polygon in the study area from 2016 to 2018.

(0.25%) among all dominant soil types in this study (Table 1), the Orangeburg sandy loam (i.e., OrA, OrB, and OrC) was found in a majority of the nitrogen-deficient polygons. These soil types accounted for 76.3% of polygons with at least a medium level of nitrogen deficiency in 2018. Specifically, OrA contributed to the 77.1% of the polygons with extremely high nitrogen deficiency. Moreover, we compared the total nitrogen budgets between the most nitrogen deficient OrA scenarios and the scenarios with the same rotation but different soil types (Table S8). For each rotation, OrA related scenarios had less nitrogen mineralization and more nitrogen leaching, which are the potential causes for the nitrogen deficiency. Low organic matter content would lead to less release of organically bonded nitrogen. While OrA also has a relatively high percentage of sand in texture (80.5%) and is consequently hard to hold water and nutrient content for crop growth (Hamdi et al., 2019).

To further verify the impact of nitrogen deficiency, the simulated annual yields of four primary crops in each polygon were plotted against the corresponding annually accumulated N_{SI} from 2016 to 2018 (Fig. 8). The annual yields of cotton and peanut clearly decreased with increasing nitrogen stress. However, in a few polygons without remarkable accumulated N_{SI}, the simulated yields of these two crops were also relatively low. In those polygons, the daily N_{SI} was large over a short period at the beginning stage of crop growth. This observation is consistent with the results of previous field studies, which have indicated that the shortage

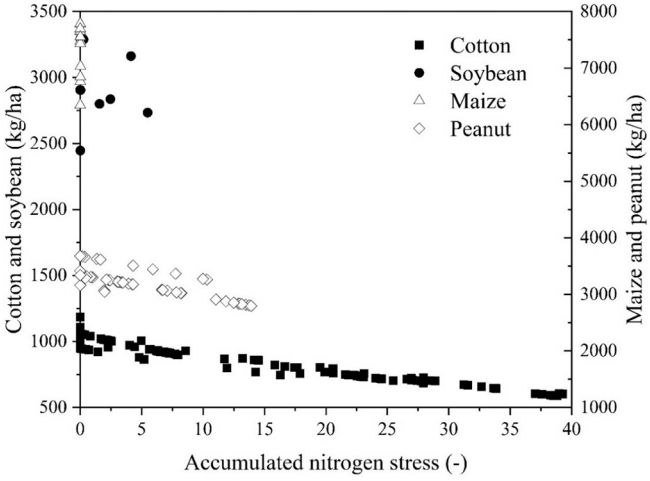

Fig. 8. Influence of accumulated nitrogen stress on the yields of the primary crops.

of nitrogen nutrient at the early growth stage would affect the canopy development, nutrient content, and final yields of crops (Ball et al., 1983; Naegle et al., 2005; Stamatiadis et al., 2006; Schlüter et al., 2012). For soybean, no clear trend could be identified between nitrogen stress and annual yields. As to maize, its annually accumulated N_{SI} was less than 0.03 in each polygon, which demonstrated that the applied nitrogen amount (i.e., 135 kg N/ha in total) was enough to support the predicted annual yields during the three years.

3.4. Yield improvement

To improve yields in identified low yield polygons, the nitrogen demand for crop growth needs to be better satisfied. Therefore, four types of management strategies to alleviate the nitrogen deficiency were tested at field scale. Although cotton and peanuts are the two most significant crops in the study area, the tests were focused on cotton yield improvement, since peanut yields were higher than the 90%, 86%, and 74% of the maximum recorded values (i.e., 3807 kg/ha) in 2016, 2017, and 2018 respectively, and were not considered as low yields. To better estimate and compare the impacts of these managements, they were only applied for the polygons having the low cotton yields in 2018 when the planted area and nitrogen deficiency of cotton both reached their highest levels.

In the first type of management, the second nitrogen fertilizer (56 kg N/ha) was applied as sidedress at different phenological stages, including germination, first square, active growth, first bloom, and grain filling, to determine the optimal timing (Fig. 9a). In the original simulation process, this sidedress was applied at the stage of active growth. The highest average yield with an increase of 4.7% was obtained when the sidedress was applied at the germination stage. When the sidedress was applied at the first square, active growth, or first blooming, the average and median of simulated yields generally declined as crops grew, though their highest yields were comparable to each other. A sharp decrease in simulated cotton yield was observed when the sidedress was applied at the grain filling. The site simulation result indicated that applying the sidedress at the germination stage could slightly improve the yields of cotton in the study area. On the contrary, a late sidedress application could lead to high nitrogen deficit at the early stage of cotton growth, which might hinder the full development of canopy, decrease the concentration of leaf chlorophyll, and therefore lower the annual yield (Radin and Boyer, 1982; Fridgen and Varco, 2004; Stamatiadis et al., 2006).

In the second type of management, the total amount of nitrogen fertilizer was gradually raised from 84 kg N/ha to 152 kg N/ha with one-third applied at the planting stage and the rest applied as sidedress at the stage of active growth (Fig. 9b). Among them, the fertilization of 84 kg N/ha was the same as the original simulation process. As more nitrogen fertilizer was applied, the simulated cotton yields increased with a shrinking interquartile range, indicating a reduction in nitrogen stress. When 152 kg N/ha of nitrogen fertilizer was applied, no nitrogen deficiency was found in the selected polygons, and the maximum cotton yield (1059 kg/ha) was reached under given conditions. Although the addition of total nitrogen fertilizer improved the average cotton yield by 74.4%, it could dramatically increase the emission of greenhouse gas (i.e., N_2O) (Huang et al., 2014; Ruan et al., 2016). Meanwhile, excessive nitrogen fertilizing might delay cotton maturity, cause rank growth, intensify insect infestations, increase the risk of boll rot, and reduce lint quality (Boquet and Breitenbeck, 2000).

In the third type of management, different combinations of nitrogen fertilizer types (i.e., ammonium and nitrate) were applied with the

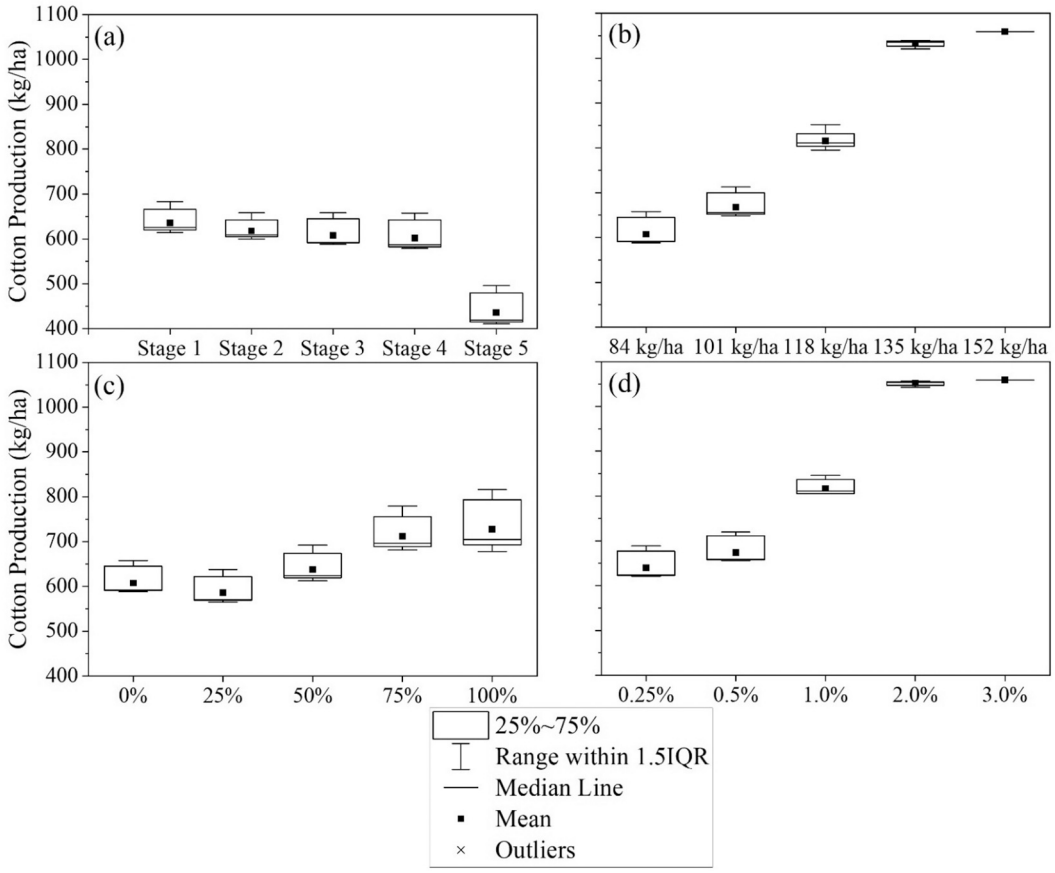

Fig. 9. Four types of management strategies to improve the simulated cotton yields in the selected polygons in 2018: (a) adjusting the application timing of sidedress, (b) increasing the total amount of nitrogen fertilizer, (c) changing the proportion of nitrate fertilizer, and (d) adjusting the content of soil organic matters.

percentage of NO_3^--N increasing from 0 to 100% (Fig. 9c). In the original simulation process, no fertilizer was applied in the form of nitrate. When the proportion of nitrate fertilizer was over 50%, the cotton yields were improved by increasing crop nitrogen uptake. Compared with the original simulation result, the average cotton yield was raised by 19.7% when nitrate was the only form of fertilizer. The improvement of simulated yields diminished after the percentage of nitrate fertilizer reached 75%, which could be an optimal strategy for nitrogen fertilization in the study area. When nitrate accounted for 25% of the applied fertilizers, the average cotton yield was 3.5% lower than the original simulation result. Even if the application of nitrate did not guarantee higher cotton yields, other advantages might be achieved through applying nitrate fertilizer, such as no volatile loss, improved uptake of cations (i.e., potassium, calcium, and magnesium), and reduced soil acidification (Haynes and Goh, 1978; Bouman et al., 1995; Sommer et al., 2004).

In the last type of management, the soil organic matter content was adjusted between the lowest (0.25%) and the highest recorded values (5.0%) in the studied area (Table S3). Specifically, this management strategy could be achieved by the application of soil amendment with high organic content such as biosolids (Cheng et al., 2007). As the soil organic matter content rose, more nitrogen was available from organic matter decomposition, which promoted the simulated cotton yields (Fig. 9d). Once the soil organic matter content reached 3.0%, the cotton yields no longer increased and all converged to the maximum value (1059 kg/ha) under given conditions. The trend of cotton yields under this type of management was similar to the result of the second type management since both managements led to more available nitrogen. However, the total soil ammonium (i.e., applied ammonium fertilizer and ammonium decomposed from soil organic matters) was 1.5 times higher under the fourth type of management, which would lead to a higher N_2O emission during the nitrification process (Sánchez-García et al., 2014).

The above four types of management strategies successfully increased the average simulated cotton yield by as high as 74.4% in the selected polygons in 2018. Each type of management had its advantages and drawback. Among them, increasing the nitrogen fertilizer amount and the soil organic matter content achieved the most significant improvement. However, these two types of management would both potentially emit more greenhouse gas (i.e., N_2O). Changing application timing of sidedress only had a trivial impact on improving cotton yields. Furthermore, a late sidedress would even cause the failure of grain filling. Switching the fertilizer type from ammonium to nitrate improved the average cotton yield by 19.7%. This management tends to reduce N_2O emission since the most important source of the nitrification process, ammonium, was replaced by nitrate and the denitrification process was usually limited under aerobic conditions. Overall, a combination of the tested management strategies should be applied to sustainably improve crop yields without having negative impacts on the environment.

3.5. Implication

Compared with previous GIS-based crop simulation, the developed framework applied more realistic crop rotations. The rotation input was very close to the real scenarios since it was directly derived from recorded agricultural land uses in each year (USDA, 2019). Taking this advantage, the simulation would contribute to a more reliable prediction and subsequently better bridge the gap between local cropping system models and the regional estimation of crop yields. On the other hand, the major limitations of the simulation came from excluding cultivar variance in the study area and pests/diseases events. The cultivar variance could be added in the simulation as another input layer if related data was available. However, the simulation may not be able to handle the pests/diseases events since the selected crop model is not equipped with related function.

4. Conclusion

By coupling a field-scale cropping system model (i.e., CropSyst, version 4) with a GIS platform (i.e., QGIS, version 3.6.3), a GIS-based framework was established in this study to simulate the primary crop yields in a cropland-concentrated USGS sub-watershed in the Geneva County, Alabama from 2016 to 2018. With well-prepared input data, crop yields were accurately predicted for dominant crops at a regional level with an overall Pearson's correlation coefficient of 0.99. The low yields polygons were identified according to the visualization of regional simulation results. Based on total nitrogen budget analysis, we found that low organic matter content and high sand percentage in texture are two potential causes for the nitrogen deficiency. And the annual cotton yield was severely impacted in 2018. Specifically, 84 cotton polygons were found having a yield in the lowest level. To address the low yields, we simulate the performance of four management strategies, which were able to increase the cotton yield by as high as 74.4%. Because of the potential negative impact (i.e., more N_2O emission), a combination of the tested management strategies should be taken to promote crop yields sustainably. This study demonstrated the ability of a GIS-based framework to simulate crop yields at a regional level.

Declaration of Competing Interest

The authors declare no conflict of interest.

Acknowledgments

The work was supported by the National Institute of Food and Agriculture of USDA through Grant No. 2018-68002-27920 to Florida A&M University and the National Science Foundation through Grant No. 1735235 to Florida A&M University as part of the National Science Foundation Research Traineeship. The authors greatly thank Roger Nelson for his advising and help in CropSyst (version 4) simulation.

Appendix A. Supplementary data

Supplementary data to this article can be found online at https://doi.org/10.1016/j.agsy.2021.103213.

References

Archontoulis, S.V., Miguez, F.E., Moore, K.J., 2014. Evaluating APSIM maize, soil water, soil nitrogen, manure, and soil temperature modules in the Midwestern United States. Agron. J. 106 (3), 1025–1040.

Balkovič, J., van der Velde, M., Schmid, E., Skalský, R., Khabarov, N., Obersteiner, M., Stürmer, B., Xiong, W., 2013. Pan-European crop modelling with EPIC: implementation, up-scaling and regional crop yield validation. Agric. Syst. 120, 61–75.

Ball, S.T., Wynne, J.C., Elkan, G.H., Schneeweis, T.J., 1983. Effect of inoculation and applied nitrogen on yield, growth and nitrogen fixation of two peanut cultivars. Field Crop Res. 6, 85–91.

Bondada, B.R., Oosterhuis, D.M., 2001. Canopy photosynthesis, specific leaf weight, and yield components of cotton under varying nitrogen supply. J. Plant Nutr. 24 (3), 469–477.

Boquet, D.J., Breitenbeck, G.A., 2000. Nitrogen rate effect on partitioning of nitrogen and dry matter by cotton. Crop Sci. 40 (6), 1685–1693.

Boquet, D.J., Hutchinson, R.L., Breitenbeck, G.A., 2004. Long-term tillage, cover crop, and nitrogen rate effects on cotton: yield and fiber properties. Agron. J. 96 (5), 1436–1442.

Bouman, O.T., Curtin, D., Campbell, C.A., Biederbeck, V.O., Ukrainetz, H., 1995. Soil acidification from long-term use of anhydrous ammonia and urea. Soil Sci. Soc. Am. J. 59 (5), 1488–1494.

Bouman, B.A.M., Van Keulen, H., Van Laar, H.H., Rabbinge, R., 1996. The 'school of de Wit' crop growth simulation models: a pedigree and historical overview. Agric. Syst. 52 (2–3), 171–198.

Cheng, H., Xu, W., Liu, J., Zhao, Q., He, Y., Chen, G., 2007. Application of composted sewage sludge (CSS) as a soil amendment for turfgrass growth. Ecol. Eng. 29 (1), 96–104.

Cherr, C.M., Scholberg, J.M.S., McSorley, R., Mbuya, O.S., 2007. Growth and yield of sweet corn following green manure in a warm temperate environment on sandy soil. J. Agron. Crop Sci. 193 (1), 1–9.

Confalonieri, R., Acutis, M., Bellocchi, G., Donatelli, M., 2009. Multi-metric evaluation of the models WARM, CropSyst, and WOFOST for rice. Ecol. Model. 220 (11), 1395–1410.
de Wit, C.T., 1958. Transpiration and crop yields (no. 64.6).
de Wit, C.T., 1965. Photosynthesis of Leaf Canopies (No. 663).
Dietrich, C., 2010. Decision making: factors that influence decision making, heuristics used, and decision outcomes. Inquiries Journal 2 (02).
Donatelli, M., Stöckle, C., Ceotto, E., Rinaldi, M., 1997. Evaluation of CropSyst for cropping systems at two locations of northern and southern Italy. Eur. J. Agron. 6 (1–2), 35–45.
Dong, H., Li, W., Eneji, A.E., Zhang, D., 2012. Nitrogen rate and plant density effects on yield and late-season leaf senescence of cotton raised on a saline field. Field Crop Res. 126, 137–144.
Dury, J., Schaller, N., Garcia, F., Reynaud, A., Bergez, J.E., 2012. Models to support cropping plan and crop rotation decisions. A review. Agronomy for Sustainable Development 32 (2), 567–580.
Dzotsi, K.A., Basso, B., Jones, J.W., 2015. Parameter and uncertainty estimation for maize, peanut and cotton using the SALUS crop model. Agric. Syst. 135, 31–47.
Farahani, H.J., Izzi, G., Oweis, T.Y., 2009. Parameterization and evaluation of the AquaCrop model for full and deficit irrigated cotton. Agron. J. 101 (3), 469–476.
Feather, P., Cooper, J.C., 1995. Voluntary incentives for reducing agricultural nonpoint source water pollution (no. 1474-2016-120850).
Florin, M.J., McBratney, A.B., Whelan, B.M., 2009. Quantification and comparison of wheat yield variation across space and time. Eur. J. Agron. 30 (3), 212–219.
Foster, W.E., Rausser, G.C., 1991. Farmer behavior under risk of failure. Am. J. Agric. Econ. 73 (2), 276–288.
Fournier, C., Andrieu, B., Ljutovac, S., Saint-Jean, S., 2003. ADEL-Wheat: A 3D Architectural Model of Wheat Development.
Fridgen, J.L., Varco, J.J., 2004. Dependency of cotton leaf nitrogen, chlorophyll, and reflectance on nitrogen and potassium availability. Agron. J. 96 (1), 63–69.
Hamdi, H., Hechmi, S., Khelil, M.N., Zoghlami, I.R., Benzarti, S., Mokni-Tlili, S., Hassen, A., Jedidi, N., 2019. Repetitive land application of urban sewage sludge: effect of amendment rates and soil texture on fertility and degradation parameters. Catena 172, 11–20.
Hansen, J.W., 1996. Is agricultural sustainability a useful concept? Agric. Syst. 50 (2), 117–143.
Hansen, J.W., Jones, J.W., 2000. Scaling-up crop models for climate variability applications. Agric. Syst. 65 (1), 43–72.
Hartkamp, A.D., White, J.W., Hoogenboom, G., 1999. Interfacing geographic information systems with agronomic modeling: a review. Agron. J. 91 (5), 761–772.
Haynes, R.J., Goh, K.M., 1978. Ammonium and nitrate nutrition of plants. Biol. Rev. 53 (4), 465–510.
Heffer, P., Prud'homme, M., 2016, December. Global Nitrogen Fertilizer Demand and Supply: Trend, Current Level and Outlook. In International Nitrogen Initiative Conference. Melbourne, Australia.
Huang, T., Gao, B., Hu, X.K., Lu, X., Well, R., Christie, P., Bakken, L.R., Ju, X.T., 2014. Ammonia-oxidation as an engine to generate nitrous oxide in an intensively managed calcareous Fluvo-aquic soil. Sci. Rep. 4, 3950.
Isen, A.M., Means, B., Patrick, R., Nowicki, G., 1982. Some factors influencing decision making strategy and risk-taking. In: Affect and Cognition: The 17th Annual Carnegie Mellon Symposium on Cognition. Erlbaum, Hillsdale, NJ, pp. 241–261.
Jin, X., Li, Z., Yang, G., Yang, H., Feng, H., Xu, X., Wang, J., Li, X., Luo, J., 2017. Winter wheat yield estimation based on multi-source medium resolution optical and radar imaging data and the AquaCrop model using the particle swarm optimization algorithm. ISPRS J. Photogramm. Remote Sens. 126, 24–37.
Jones, J.W., Antle, J.M., Basso, B., Boote, K.J., Conant, R.T., Foster, I., Godfray, H.C.J., Herrero, M., Howitt, R.E., Janssen, S., Keating, B.A., 2017. Brief history of agricultural systems modeling. Agric. Syst. 155, 240–254.
Kadiyala, M.D.M., Nedumaran, S., Singh, P., Chukka, S., Irshad, M.A., Bantilan, M.C.S., 2015. An integrated crop model and GIS decision support system for assisting agronomic decision making under climate change. Sci. Total Environ. 521, 123–134.
Kissel, D.E., Sonon, L., 2008. Fertilizer recommendations by crops, categorized. Soil Test Handbook for Georgia 90–616.
Kollas, C., Kersebaum, K.C., Nendel, C., Manevski, K., Müller, C., Palosuo, T., Armas-Herrera, C.M., Beaudoin, N., Bindi, M., Charfeddine, M., Conradt, T., 2015. Crop rotation modelling—A European model intercomparison. Eur. J. Agron. 70, 98–111.
Liu, J., 2009. A GIS-based tool for modelling large-scale crop-water relations. Environ. Model Softw. 24 (3), 411–422.
Liu, H.L., Yang, J.Y., Drury, C.A., Reynolds, W.D., Tan, C.S., Bai, Y.L., He, P., Jin, J., Hoogenboom, G., 2011. Using the DSSAT-CERES-maize model to simulate crop yield and nitrogen cycling in fields under long-term continuous maize production. Nutr. Cycl. Agroecosyst. 89 (3), 313–328.
Maguire, D.J., 1991. An overview and definition of GIS. Geographical information systems: Principles and applications, 1, pp. 9–20.
Morari, F., Lugato, E., Borin, M., 2004. An integrated non-point source model-GIS system for selecting criteria of best management practices in the Po Valley, North Italy. Agric. Ecosyst. Environ. 102 (3), 247–262.
Moriasi, D.N., Arnold, J.G., Van Liew, M.W., Bingner, R.L., Harmel, R.D., Veith, T.L., 2007. Model evaluation guidelines for systematic quantification of accuracy in watershed simulations. Trans. ASABE 50 (3), 885–900.
Naegle, E.R., Burton, J.W., Carter, T.E., Rufty, T.W., 2005. Influence of seed nitrogen content on seedling growth and recovery from nitrogen stress. Plant Soil 271 (1–2), 329–340.
NASS, U., 2010. Field crops: Usual planting and harvesting dates. USDA National Agricultural Statistics Service, Agricultural Handbook, p. 628.
NRCS, N., 2017. Conservation Practice Standard. http://www.nrcs.usda.gov.
Ortiz, B.V., Hoogenboom, G., Vellidis, G., Boote, K., Davis, R.F., Perry, C., 2009. Adapting the CROPGRO-cotton model to simulate cotton biomass and yield under southern root-knot nematode parasitism. Trans. ASABE 52 (6), 2129–2140.
Parker, D.C., Manson, S.M., Janssen, M.A., Hoffmann, M.J., Deadman, P., 2003. Multi-agent systems for the simulation of land-use and land-cover change: a review. Ann. Assoc. Am. Geogr. 93 (2), 314–337.
Parry, M.L., Rosenzweig, C., Iglesias, A., Livermore, M., Fischer, G., 2004. Effects of climate change on global food production under SRES emissions and socio-economic scenarios. Glob. Environ. Chang. 14 (1), 53–67.
Parton, W.J., Hartman, M., Ojima, D., Schimel, D., 1998. DAYCENT and its land surface submodel: description and testing. Glob. Planet. Chang. 19 (1–4), 35–48.
Perez, M.R., 2015. Regulating farmer nutrient management: a three-state case study on the Delmarva Peninsula. J. Environ. Qual. 44 (2), 402–414.
Pradal, C., Dufour-Kowalski, S., Boudon, F., Fournier, C., Godin, C., 2008. OpenAlea: a visual programming and component-based software platform for plant modelling. Funct. Plant Biol. 35 (10), 751–760.
Priya, S., Shibasaki, R., 2001. National spatial crop yield simulation using GIS-based crop production model. Ecol. Model. 136 (2–3), 113–129.
QGIS Development Team, 2016. QGIS Geographic Information System. Open source geospatial foundation project.
Radin, J.W., Boyer, J.S., 1982. Control of leaf expansion by nitrogen nutrition in sunflower plants: role of hydraulic conductivity and turgor. Plant Physiol. 69 (4), 771–775.
Resop, J.P., Fleisher, D.H., Wang, Q., Timlin, D.J., Reddy, V.R., 2012. Combining explanatory crop models with geospatial data for regional analyses of crop yield using field-scale modeling units. Comput. Electron. Agric. 89, 51–61.
Ruan, L., Bhardwaj, A.K., Hamilton, S.K., Robertson, G.P., 2016. Nitrogen fertilization challenges the climate benefit of cellulosic biofuels. Environmental research letters 11 (6), 064007.
Sánchez-García, M., Roig, A., Sánchez-Monedero, M.A., Cayuela, M.L., 2014. Biochar increases soil N2O emissions produced by nitrification-mediated pathways. Frontiers in Environmental Science 2, 25.
Schlüter, U., Mascher, M., Colmsee, C., Scholz, U., Bräutigam, A., Fahnenstich, H., Sonnewald, U., 2012. Maize source leaf adaptation to nitrogen deficiency affects not only nitrogen and carbon metabolism but also control of phosphate homeostasis. Plant Physiol. 160 (3), 1384–1406.
Setiyono, T.D., Cassman, K.G., Specht, J.E., Dobermann, A., Weiss, A., Yang, H., Conley, S.P., Robinson, A.P., Pedersen, P., De Bruin, J.L., 2010. Simulation of soybean growth and yield in near-optimal growth conditions. Field Crop Res. 119 (1), 161–174.
Smith, L.E., Siciliano, G., 2015. A comprehensive review of constraints to improved management of fertilizers in China and mitigation of diffuse water pollution from agriculture. Agric. Ecosyst. Environ. 209, 15–25.
Soil Survey Staff, 2019. Natural Resources Conservation Service, United States Department of Agriculture. Soil Survey Geographic (SSURGO) Database for [Alabama] (Available online. Accessed [May/17/2019]).
Sommer, S.G., Schjoerring, J.K., Denmead, O.T., 2004. Ammonia emission from mineral fertilizers and fertilized crops. Adv. Agron. 82 (557622) (82008–4).
Sommer, R., Kienzler, K., Conrad, C., Ibragimov, N., Lamers, J., Martius, C., Vlek, P., 2008. Evaluation of the CropSyst model for simulating the potential yield of cotton. Agronomy for SustainableD development 28 (2), 345–354.
Stamatiadis, S., Christofides, C., Tsadilas, C., Samaras, V., Schepers, J.S., 2006. Natural abundance of foliar 15N as an early indicator of nitrogen deficiency in fertilized cotton. J. Plant Nutr. 29 (1), 113–125.
Stöckle, C.O., Donatelli, M., Nelson, R., 2003. CropSyst, a cropping systems simulation model. Eur. J. Agron. 18 (3–4), 289–307.
Stuart, D., Schewe, R.L., McDermott, M., 2014. Reducing nitrogen fertilizer application as a climate change mitigation strategy: understanding farmer decision-making and potential barriers to change in the US. Land Use Policy 36, 210–218.
Thornton, P.E., Thornton, M.M., Mayer, B.W., Wei, Y., Devarakonda, R., Vose, R.S., Cook, R.B., 2018. Daymet: daily surface weather data on a 1-km grid for North America, version 3. ORNL DAAC, Oak Ridge, Tennessee, USA. https://doi.org/10.3334/ORNLDAAC/1328.
Thorp, K.R., DeJonge, K.C., Kaleita, A.L., Batchelor, W.D., Paz, J.O., 2008. Methodology for the use of DSSAT models for precision agriculture decision support. Comput. Electron. Agric. 64 (2), 276–285.
Todorovic, M., Albrizio, R., Zivotic, L., Saab, M.T.A., Stöckle, C., Steduto, P., 2009. Assessment of AquaCrop, CropSyst, and WOFOST models in the simulation of sunflower growth under different water regimes. Agron. J. 101 (3), 509–521.
U.S. Geological Survey, 2019. National Hydrography Dataset (ver. USGS National Hydrography Dataset Best Resolution (NHD) for Hydrologic Unit (HU) 4–2001 (published 20191002)). accessed October 23, 2019 at URL. https://www.usgs.gov/core-science-systems/ngp/national-hydrography/access-national-hydrography-products.
USDA National Agricultural Statistics Service Cropland Data Layer, . ublished crop-specific data layer [Online]. Available at. https://nassgeodata.gmu.edu/CropScape/. accessed May 17, 2019. USDA-NASS, Washington, DC.
USDA-NASS, 2003. USDA National Agricultural Statistics Service.
Yang, J.M., Yang, J.Y., Liu, S., Hoogenboom, G., 2014. An evaluation of the statistical methods for testing the performance of crop models with observed data. Agric. Syst. 127, 81–89.
Zhang, Y., Li, C., Zhou, X., Moore III, B., 2002. A simulation model linking crop growth and soil biogeochemistry for sustainable agriculture. Ecol. Model. 151 (1), 75–108.
Zhang, X., Izaurralde, R.C., Manowitz, D., West, T.O., Post, W.M., Thomson, A.M., Bandaru, V.P., Nichols, J., Williams, J.R., 2016. An integrative modeling framework

to evaluate the productivity and sustainability of biofuel crop production systems. Gcb Bioenergy 2 (5), 258–277.
Zhang, B., Feng, G., Read, J.J., Kong, X., Ouyang, Y., Adeli, A., Jenkins, J.N., 2016. Simulating soybean productivity under rainfed conditions for major soil types using APEX model in east Central Mississippi. Agric. Water Manag. 177, 379–391.
Zhang, M., Wang, L., Wan, Y., Liu, F., Zhang, K., 2017. Rational nitrogen strategies can improve Peanut source supply capacity and pod yield. Agron. J. 109 (6), 2927–2935.